



ELSEVIER

Physics Letters B 544 (2002) 97–112

---

---

PHYSICS LETTERS B

---

---

[www.elsevier.com/locate/npe](http://www.elsevier.com/locate/npe)

# A precision measurement of direct CP violation in the decay of neutral kaons into two pions

J.R. Batley, R.S. Dosanjh, T.J. Gershon<sup>1</sup>, G.E. Kalmus, C. Lazzeroni, D.J. Munday, E. Olaiya, M. Patel, M.A. Parker, T.O. White, S.A. Wotton

*Cavendish Laboratory, University of Cambridge, Cambridge, CB3 0HE, UK<sup>2</sup>*

R. Arcidiacono, G. Barr, G. Bocquet, A. Ceccucci, T. Cuhadar-Dönszelmann, D. Cundy, N. Doble, V. Falaleev, L. Gatignon, A. Gonidec, B. Gorini, P. Grafström, W. Kubischta, I. Mikulec<sup>3</sup>, A. Norton, S. Palestini, B. Panzer-Steindel, D. Schinzel, H. Wahl

*CERN, CH-1211 Genève 23, Switzerland*

C. Cheshkov, P. Hristov, V. Kekelidze, D. Madigojine, N. Molokanova, Yu. Potrebenikov, A. Zinchenko

*Joint Institute for Nuclear Research, Dubna, Russia*

P. Rubin<sup>4</sup>, R. Sacco, A. Walker

*Department of Physics and Astronomy, University of Edinburgh, Edinburgh, EH9 3JZ, UK<sup>2</sup>*

D. Bettoni, R. Calabrese, P. Dalpiaz, J. Duclos, P.L. Frabetti<sup>5</sup>, A. Gianoli, M. Martini, L. Masetti, F. Petrucci, M. Savrié, M. Scarpa

*Dipartimento di Fisica dell'Università e Sezione dell'INFN di Ferrara, I-44100 Ferrara, Italy*

A. Bizzeti<sup>6</sup>, M. Calvetti, G. Collazuol, E. Iacopini, M. Lenti, F. Martelli<sup>7</sup>, G. Ruggiero, M. Veltri<sup>7</sup>

*Dipartimento di Fisica dell'Università e Sezione dell'INFN di Firenze, I-50125 Firenze, Italy*

D. Coward, M. Eppard, A. Hirstius, K. Holtz, K. Kleinknecht, U. Koch, L. Köpke, P. Lopes da Silva, P. Marouelli, I. Mestvirishvili, C. Morales, I. Pellmann, A. Peters,

**B. Renk, S.A. Schmidt, V. Schönharting, R. Wanke, A. Winhart**

*Institut für Physik, Universität Mainz, D-55099 Mainz, Germany<sup>8</sup>*

**J.C. Chollet, L. Fayard, G. Graziani, L. Iconomidou-Fayard, G. Unal, I. Wingerter-Seez**

*Laboratoire de l'Accélérateur Linéaire, IN2P3-CNRS, Université de Paris-Sud, 91898 Orsay, France<sup>9</sup>*

**G. Anzivino, P. Cenci, E. Imbergamo, G. Lamanna, P. Lubrano, A. Mestvirishvili,  
A. Nappi, M. Pepe, M. Piccini, M. Valdata-Nappi**

*Dipartimento di Fisica dell'Università e Sezione dell'INFN di Perugia, I-06100 Perugia, Italy*

**R. Casali, C. Cerri, M. Cirilli<sup>10</sup>, F. Costantini, R. Fantechi, L. Fiorini, S. Giudici,  
I. Mannelli, G. Pierazzini, M. Sozzi**

*Dipartimento di Fisica, Scuola Normale Superiore e Sezione dell'INFN di Pisa, I-56100 Pisa, Italy*

**J.B. Cheze, M. De Beer, P. Debu, F. Derue, A. Formica, G. Gouge, G. Marel,  
E. Mazzucato, B. Peyaud, R. Turlay, B. Vallage**

*DSM/DAPNIA - CEA Saclay, F-91191 Gif-sur-Yvette, France*

**M. Holder, A. Maier, M. Ziolkowski**

*Fachbereich Physik, Universität Siegen, D-57068 Siegen, Germany<sup>11</sup>*

**C. Biino, N. Cartiglia, M. Clemencic, F. Marchetto, E. Menichetti, N. Pastrone**

*Dipartimento di Fisica Sperimentale dell'Università e Sezione dell'INFN di Torino, I-10125 Torino, Italy*

**J. Nassalski, E. Rondio, W. Wislicki, S. Wronka**

*Soltan Institute for Nuclear Studies, Laboratory for High Energy Physics, PL-00-681 Warsaw, Poland<sup>12</sup>*

**H. Dibon, M. Jeitler, M. Markytan, G. Neuhofer, M. Pernicka, A. Taurok, L. Widhalm**

*Österreichische Akademie der Wissenschaften, Institut für Hochenergiephysik, A-1050 Wien, Austria<sup>13</sup>*

Received 25 July 2002; accepted 30 July 2002

## Abstract

The direct CP violation parameter  $\text{Re}(\epsilon'/\epsilon)$  has been measured from the decay rates of neutral kaons into two pions using the NA48 detector at the CERN SPS. The 2001 running period was devoted to collecting additional data under varied conditions compared to earlier years (1997–1999). The new data yield the result:  $\text{Re}(\epsilon'/\epsilon) = (13.7 \pm 3.1) \times 10^{-4}$ . Combining this result with that published from the 1997, 98 and 99 data, an overall value of  $\text{Re}(\epsilon'/\epsilon) = (14.7 \pm 2.2) \times 10^{-4}$  is obtained from the NA48 experiment.

© 2002 Elsevier Science B.V. All rights reserved.

## 1. Introduction

CP violation was discovered 38 years ago in the decays of neutral kaons [1]. Recently CP violation in the  $B^0$  mesons has also been observed [2]; nevertheless neutral kaons remain a privileged system for the study of the phenomenon.

CP conservation would imply that the  $K_S$  and  $K_L$  particles are pure CP-eigenstates and that  $K_L$  decay only into CP = -1 and  $K_S$  into CP = +1 final states. The observed signal of the forbidden  $K_L \rightarrow 2\pi$  decays (CP = +1) indicates that CP is not a conserved symmetry.

CP violation can occur via the mixing of CP eigenstates, called *indirect* CP violation, represented by the parameter  $\epsilon$ . CP violation can also occur in the decay process through the interference of amplitudes with different isospins. This is represented by the parameter  $\epsilon'$  and is called *direct* CP violation.

In the Standard Model of electro-weak interaction, CP violation is naturally accommodated by an irreducible complex phase in the quark mixing-matrix [3]. Current theoretical predictions of  $\epsilon'/\epsilon$  range  $\sim -10 \times 10^{-4}$  to  $\sim +30 \times 10^{-4}$  [4].

Experimentally, it is convenient to measure the double ratio  $R$  of decay widths, which is related to the ratio  $\epsilon'/\epsilon$  as follows:

$$R = \frac{\Gamma(K_L \rightarrow \pi^0\pi^0)}{\Gamma(K_S \rightarrow \pi^0\pi^0)} \bigg/ \frac{\Gamma(K_L \rightarrow \pi^+\pi^-)}{\Gamma(K_S \rightarrow \pi^+\pi^-)} \approx 1 - 6 \times \text{Re}(\epsilon'/\epsilon). \quad (1)$$

In 1993, two experiments published their final results: NA31 [5] measured  $\text{Re}(\epsilon'/\epsilon) = (23.0 \pm 6.5) \times 10^{-4}$ , and the result of E731 [6] was  $\text{Re}(\epsilon'/\epsilon) = (7.4 \pm 5.9) \times 10^{-4}$ . Recently, two experiments announced results from samples of their total statistics. NA48 published a result of  $\text{Re}(\epsilon'/\epsilon) = (15.3 \pm 2.6) \times 10^{-4}$ , using data collected in 1997 [7], 1998 and 99 [8], and KTeV presented a preliminary result of  $\text{Re}(\epsilon'/\epsilon) = (20.7 \pm 2.8) \times 10^{-4}$  [9] on data accumulated in 1996 [10] and 97. These observations con-

*E-mail address:* heinrich.wahl@cern.ch (H. Wahl).

<sup>1</sup> Present address: High Energy Accelerator Research Organization (KEK), Tsukuba, Ibaraki, 305-0801, Japan.

<sup>2</sup> Funded by the UK Particle Physics and Astronomy Research Council.

<sup>3</sup> On leave from Österreichische Akademie der Wissenschaften, Institut für Hochenergiephysik, A-1050 Wien, Austria.

<sup>4</sup> Permanent address: Department of Physics, University of Richmond, VA 27313, USA.

<sup>5</sup> Dipartimento di Fisica e INFN Bologna, viale Berti-Pichat 6/2, I-40127 Bologna, Italy.

<sup>6</sup> Dipartimento di Fisica dell'Università di Modena e Reggio Emilia, via G. Campi 213/A I-41100, Modena, Italy.

<sup>7</sup> Istituto di Fisica Università di Urbino.

<sup>8</sup> Funded by the German Federal Minister for Research and Technology (BMBF) under contract 7MZ18P(4)-TP2.

<sup>9</sup> Funded by Institut National de Physique des Particules et de Physique Nucléaire (IN2P3), France.

<sup>10</sup> Present address: Dipartimento di Fisica dell'Università di Roma "La Sapienza" e Sezione INFN di Roma, I-00185 Roma, Italy.

<sup>11</sup> Funded by the German Federal Minister for Research and Technology (BMBF) under contract 056SI74.

<sup>12</sup> Supported by the Committee for Scientific Research grants 5P03B10120, 2P03B11719 and SPUB-M/CERN/P03/DZ210/2000 and using computing resources of the Interdisciplinary Center for Mathematical and Computational Modelling of the University of Warsaw.

<sup>13</sup> Funded by the Austrian Ministry of Education, Science and Culture under contract GZ 616.360/2-IV GZ 616.363/2-VIII, and by the Fund for Promotion of Scientific Research in Austria (FWF) under contract P08929-PHY.

firmed the existence of a direct CP-violation component.

This Letter reports a measurement of  $\text{Re}(\epsilon'/\epsilon)$  performed using the 2001 data sample, recorded in somewhat different experimental conditions by the NA48 experiment.

After the 1999 data-taking period, the drift chambers of the experiment were damaged by the implosion of the beam tube. The data taking in 2001 took place with rebuilt drift chambers. Thanks to the possibility of a better SPS duty cycle, increased by a factor 1.8 with respect to the 1998–1999 running period, the data could be taken at a 30% lower beam intensity, allowing the insensitivity of the result to intensity-related effects to be checked, and the statistics for the final  $\epsilon'/\epsilon$  measurement by NA48 to be completed. The statistics accumulated during the 93 days of the 2001 data-taking period is roughly half of the total statistics accumulated in the 263 days of the 1998 and 1999 periods.

Details of the apparatus and of the data analysis can be found in [8], here only the differences with respect to the 1998–1999 data-taking will be stressed.

## 2. The method

$\text{Re}(\epsilon'/\epsilon)$  is derived from the double ratio  $R$ . The experiment is designed to exploit cancellations of systematic effects contributing symmetrically to different components of the double ratio.

The four decay modes are collected simultaneously, which minimises the sensitivity of the measurement to accidental activity and to variations in beam intensity and detection efficiency. In the analysis  $K_S$  events are further weighted by the  $K_L/K_S$  intensity ratio to eliminate the small and slow variations of the  $K_L$  and  $K_S$  beam intensities. To maintain the simultaneous data-taking of  $\pi^0\pi^0$  and  $\pi^+\pi^-$  decays, dead-time conditions affecting one mode are recorded and applied offline in all modes.

$K_L$  and  $K_S$  decays are provided by two nearly-collinear beams with similar momentum spectra, converging to the centre of the main detector. The same decay region is used for all modes. In order to minimise the acceptance correction due to the difference in mean decay lengths,  $K_L$  decays are weighted as a function of their proper lifetime, such that the  $K_L$

decay distribution becomes similar to that of  $K_S$ . In this way, the accuracy of the result does not rely on a detailed Monte Carlo simulation of the experiment and only small remaining differences in beam divergences and geometries need to be corrected using Monte Carlo simulation. To be insensitive to residual differences in the beam momentum spectra, the analysis is performed in bins of kaon energy.

$K_S$  decays are distinguished from  $K_L$  decays by a coincidence between the decay time and the registered times of the protons producing the  $K_S$  beam. As the same method is used for  $\pi^+\pi^-$  and  $\pi^0\pi^0$  decays, the double ratio is sensitive only to differences in misidentification probabilities between the two decay modes and not to their absolute values.

Finally, high-resolution detectors are used to detect the  $\pi^+\pi^-$  and  $\pi^0\pi^0$  final states in order to minimise residual backgrounds which do not cancel in the double ratio.

## 3. Beams and detectors

### 3.1. Beams

The  $K_L$  and  $K_S$  beams [11] are produced in two different targets by protons from the same CERN SPS beam. In the 2001 run the SPS had a cycle time of 16.8 s with a spill length of 5.2 s and a proton momentum of 400 GeV/c.<sup>14</sup> Since the  $K_S$  and  $K_L$  beams are produced concurrently, the  $K_S/K_L$  ratio is maintained stable to within  $\pm 10\%$ .

The primary, high-flux proton beam ( $\sim 2.4 \times 10^{12}$  protons per pulse) impinges on the  $K_L$  target (a 400 mm long, 2 mm diameter rod of beryllium), with an incidence angle of 2.4 mrad relative to the  $K_L$  beam axis. The charged component of the outgoing particles is swept away by bending magnets. The neutral beam passes through three stages of collimation and the fiducial region starts at the exit of the “final” collimator, 126 m downstream of the target. At this point, this neutral beam is dominated by long-lived kaons, neutrons and photons; only small

<sup>14</sup> The cycle time was 14.4 s, the spill length 2.38 s and the proton momentum 450 GeV/c in the 1998 and 1999 runs. The effective spill length, given by the remaining time structures in the beam is  $\approx 3.6$  s in 2001, compared to  $\approx 1.7$  s for the 1998–1999 data.

fractions of the most energetic short-lived components ( $K_S$  and  $\Lambda$ ) survive.

The protons not interacting in the  $K_L$  target are directed onto a mechanically bent mono-crystal of silicon [12]. A small fraction of protons satisfies the conditions for channelling and is bent to produce a collimated beam of  $\sim 5 \times 10^7$  protons per pulse, which is then deflected back onto the  $K_L$  beam axis and finally directed to the  $K_S$  target (of similar dimensions as the  $K_L$  target) located 72 mm above the  $K_L$  beam axis. A combination of a sweeping magnet and collimator selects a neutral beam at 4.2 mrad to the incoming protons. The decay spectrum of kaons at the exit of the collimator (6 m downstream of the target) is similar to that in the  $K_L$  beam, with an average energy of 110 GeV.<sup>15</sup> Two-pion decays from this beam come almost exclusively from  $K_S$  decays.

The tagging station (Tagger) is located on the path of the  $K_S$  proton beam after the bent crystal. It consists of two ladders of 12 scintillator strips each, covering the beam horizontally and vertically [13]. A proton crosses at least two scintillators, one horizontal and one vertical. The reconstructed time per counter has a resolution of  $\sim 140$  ps, and two pulses 4–5 ns apart can be resolved.

The beginning of the  $K_S$  decay region is sharply defined by an anticounter (AKS), located at the exit of the  $K_S$  collimator [14]. It is composed of a photon converter followed by three scintillator counters. Its main purpose is to veto all upstream decays from the  $K_S$  beam.

The decay region is contained in an evacuated ( $< 3 \times 10^{-5}$  mbar) 90 m long tank with a 0.9 mm (0.003 radiation length) thick polyamide (Kevlar) composite window at the end. The neutral beam continues in a 16 cm diameter evacuated tube to the beam dump, downstream of all detector elements.

### 3.2. Detectors

Charged particles from decays are measured by a magnetic spectrometer [15] composed of four drift

chambers with a dipole magnet (inducing a transverse momentum-kick of 265 MeV/c in the horizontal plane) between the second and third chambers. These chambers and their interconnecting beam tube are aligned along the bisector between the converging  $K_S$  and  $K_L$  beam axes. Each chamber is comprised of eight planes of sense wires, two horizontal, two vertical and two along each of the  $45^\circ$  directions. In the third chamber, only the horizontal and vertical planes are instrumented. The average efficiency per plane is 99.5%, with a radial uniformity better than  $\pm 0.2\%$ . The space point resolution is  $\approx 95 \mu\text{m}$ . The momentum resolution is  $\sigma(p)/p = 0.48\% \oplus 0.009\% \times p$ , where the momentum  $p$  is in GeV/c. These performance figures are similar to those obtained previously [8].

The magnetic spectrometer is followed by a scintillator hodoscope, composed of two planes segmented in horizontal and vertical strips. Fast logic combines the strip signals (arranged in four quadrants) for use in the first level of the  $\pi^+\pi^-$  trigger.

A liquid krypton calorimeter (LKr) is used to reconstruct  $K \rightarrow 2\pi^0$  decays. It is a quasi-homogeneous detector with an active volume of  $\sim 10 \text{ m}^3$  of liquid Krypton. Cu–Be–Co ribbon electrodes of  $40 \mu\text{m} \times 18 \text{ mm} \times 125 \text{ cm}$  define  $\sim 13000$  cells (each with  $2 \text{ cm} \times 2 \text{ cm}$  cross-section) in a structure of longitudinal projective towers pointing to the centre of the decay region [16]. The calorimeter is 27 radiation lengths long and fully contains electromagnetic showers with energies up to 100 GeV. The energy resolution of the calorimeter is  $\sigma(E)/E = (3.2 \pm 0.2)\%/\sqrt{E} \oplus (9 \pm 1)\%/E \oplus (0.42 \pm 0.05)\%$  with  $E$  in GeV [17]. The LKr calorimeter also is used, together with an iron-scintillator calorimeter, to measure the total deposited energy for triggering purposes.

Finally, at the end of the beam line, muon counters are used to identify  $K_L \rightarrow \pi\mu\nu(K_{\mu 3})$  decays.

Two beam counters are used to measure the intensity of the beams: one is located at the extreme end of the  $K_L$  beam line ( $K_L$  monitor) and the other ( $K_S$  monitor) views the  $K_S$  target station. For the 2001 data taking, another  $K_L$  monitor with a higher counting rate was added and a  $K_S$  monitor near the tagging station was installed. These allow better measurements of the beam structures to be made down to a time scale of  $\approx 200$  ns.

<sup>15</sup> Despite the different proton momentum in the 1998 and 1999 runs, the  $K_L$  and  $K_S$  spectra remain similar, depending only on the choice of production angles to compensate for the length of the  $K_S$  collimator.

### 3.3. Triggers

The rate of particles reaching the detector is around 400 kHz. The trigger is designed to reduce this rate to less than 10 kHz, with minimal loss from dead time and inefficiencies. A part of the read-out rate is reserved for redundant low-bias triggers that collect data used for the direct determination of the trigger inefficiencies.

Triggers initiated by the beam monitors are used to record the accidental activity, with rates proportional to  $K_L$  and  $K_S$  decay rates. Beam monitor signals are down-scaled and delayed by  $69\ \mu\text{s}$  corresponding to the periodicity of the slow proton extraction (3 SPS revolutions).

#### 3.3.1. Trigger for $\pi^0\pi^0$ decays

The trigger for  $\pi^0\pi^0$  decays [18] operates digitally on the analogue sums of signals from  $2 \times 8$  cells (in both horizontal and vertical orientations) of the LKr calorimeter. These sums are converted into kinematic quantities by a “look-up table” system.

The trigger requires an electro-magnetic energy deposit greater than 50 GeV, a centre of energy (distance between the extrapolated kaon impact point at the calorimeter plane and the beam axis) smaller than 25 cm, and a decay vertex less than  $5 K_S$  lifetimes ( $\tau_S$ ) from the beginning of the decay volume. Requesting less than 6 peaks within 9 ns in both projections helps to reject background from  $K_L \rightarrow 3\pi^0$  (this condition is released if accidental activity is detected close in time).

A trigger for  $3\pi^0$  decays, given by the down-scaled  $\pi^0\pi^0$  trigger without the peak condition, is used for tagging studies.

#### 3.3.2. Trigger for $\pi^+\pi^-$ decays

The  $\pi^+\pi^-$  decays are triggered with a two-level trigger system. At the first level, the rate is reduced to 100 kHz by a coincidence of three fast signals: opposite quadrant coincidence in the scintillator hodoscope ( $Q_x$ ), hit multiplicity in the first drift chamber integrated over 200 ns, and the total calorimetric energy ( $E_{\text{tot}}$ , with a threshold of 35 GeV).

The second level of the  $\pi^+\pi^-$  trigger [19], consisting of hardware coordinate builders and a farm of asynchronous microprocessors, reconstructs tracks using data from the drift chambers. Triggers are accepted

if the tracks converge to within 5 cm, their opening angle is smaller than 15 mrad, the reconstructed proper decay time is smaller than  $4.5 \tau_S$  and the reconstructed  $\pi\pi$  mass is greater than  $0.95 m_K$ .

## 4. Event reconstruction and selection

### 4.1. $\pi^0\pi^0$

$K \rightarrow \pi^0\pi^0$  decays are selected using only data from the LKr calorimeter. The reconstruction of photon showers and the details of the small corrections applied to the energy and position measurements can be found in [8] and [20]. Photon showers in the energy range 3–100 GeV are used. Fiducial cuts are applied to ensure that the photon energies are well measured: the shower position should be more than 15 cm away from the axis of the beam tube, more than 11 cm away from the outer edges of the calorimeter and more than 2 cm away from a defective calorimeter channel ( $\approx 0.4\%$  of the channels).  $\pi^0\pi^0$  decays are selected by requiring four showers which are reconstructed within  $\pm 5$  ns of their average time and fulfill the cuts above. The minimum distance between photons is required to be more than 10 cm. To reduce the background from  $K_L \rightarrow 3\pi^0$  decays, events are rejected which have an additional cluster of energy above 1.5 GeV and within  $\pm 3$  ns of the time of the  $\pi^0\pi^0$  candidate.

From the measured photon energies  $E_i$  and impact point positions on the calorimeter  $x_i, y_i$ , the distance  $D$  from the decay vertex to the calorimeter is computed as follows, assuming that the invariant mass of the four showers is the kaon mass ( $m_K$ ):

$$D = \frac{\sqrt{\sum_i \sum_{j>i} E_i E_j ((x_i - x_j)^2 + (y_i - y_j)^2)}}{m_K}. \quad (2)$$

The average resolution on the decay vertex position is about 55 cm, and the resolution on the kaon energy is  $\approx 0.5\%$ .

The invariant masses  $m_1$  and  $m_2$  of the two photon pairs are computed using  $D$  and compared to the nominal  $\pi^0$  mass ( $m_{\pi^0}$ ). For this, the following  $\chi^2$  variable is constructed:

$$\chi^2 = \left[ \frac{(m_1 + m_2)/2 - m_{\pi^0}}{\sigma_+} \right]^2 + \left[ \frac{(m_1 - m_2)/2}{\sigma_-} \right]^2. \quad (3)$$

The mass combinations  $m_1 + m_2$  and  $m_1 - m_2$  are to good approximation uncorrelated.  $\sigma_+$  and  $\sigma_-$  are the resolutions of  $(m_1 + m_2)/2$  and  $(m_1 - m_2)/2$  parameterised from the data as a function of the lowest photon energy. Typical values of  $\sigma_+$  and  $\sigma_-$  are 0.4 and 0.8 MeV/ $c^2$ . Out of the three possible photon pairings, the one with the lowest  $\chi^2$  value is kept. To select good  $\pi^0\pi^0$  candidates and reject the residual background from  $K_L \rightarrow 3\pi^0$  decays, the cut  $\chi^2 < 13.5$  is applied.

The event time is computed by combining eight time estimators from the two most energetic cells of each cluster. An average resolution of 220 ps is thereby obtained.

#### 4.2. $\pi^+\pi^-$

The  $\pi^+\pi^-$  events are reconstructed from tracks using hits in the drift chambers of the spectrometer; the track momenta are calculated using the measured magnetic field map and alignment constants.

A vertex position is calculated for each pair of tracks with opposite charge after correcting for the small residual magnetic field due to the magnetisation of the vacuum tank ( $\sim 2 \times 10^{-3}$  Tm). The average resolution on the longitudinal vertex position is about 50 cm, whereas the transverse position resolution is around 2 mm. Since the beams are separated vertically by about 6 cm in the decay region, a clean identification of  $K_S$  and  $K_L$  decays is possible using the reconstructed vertex position.

Only tracks with momenta greater than 10 GeV/ $c$  and not closer than 12 cm to the centre of each chamber are accepted. The separation of the two tracks at their closest approach is required to be less than 3 cm. The track positions, extrapolated downstream, are required to be within the acceptance of the LKr calorimeter and of the muon veto system, in order to ensure proper electron and muon identification.

The kaon energy is computed from the opening angle  $\theta$  of the two tracks upstream of the magnet and from the ratio of their momenta  $p_1$  and  $p_2$ , assuming a  $K \rightarrow \pi^+\pi^-$  decay:

$$E_K = \sqrt{\frac{\mathcal{R}}{\theta^2} (m_K^2 - \mathcal{R}m_\pi^2)},$$

$$\text{where } \mathcal{R} = \frac{p_1}{p_2} + \frac{p_2}{p_1} + 2. \quad (4)$$

This measurement of the kaon energy is independent of the absolute magnetic field and relies mostly on the knowledge of the geometry of the detector.

A variable  $\mathcal{A}$  related to the decay orientation in the kaon rest frame is defined as  $\mathcal{A} = |p_1 - p_2|/(p_1 + p_2)$ . A cut is applied to  $\mathcal{A}$  ( $\mathcal{A} < \min(0.62, 1.08 - 0.0052 \times E_K)$ , where  $E_K$  is in GeV), to remove asymmetric decays in which one of the tracks could be close to the beam tube where the Monte Carlo modelling is more critical. This cut also removes  $\Lambda \rightarrow p\pi^-$  decays.

To reject background from semileptonic  $K_L$  decays, events with tracks consistent with being either an electron or a muon are rejected. To identify electrons, the ratio  $E/p$  of the energy of the matching cluster in the LKr calorimeter to the track momentum is computed. Pion candidate tracks are required to satisfy  $E/p < 0.8$ . Tracks are identified as muons if hits are found in time in the muon counters near the extrapolated track impact point.

For good  $\pi^+\pi^-$  events, the reconstructed mass  $m_{\pi\pi}$  should be consistent with the kaon mass. The resolution on the invariant mass  $\sigma_m$  is typically 2.5 MeV/ $c^2$ . An energy-dependent cut at  $\pm 3\sigma_m$  is applied. A further reduction of background from semileptonic decays is achieved with a cut based on the transverse momentum of the kaon. To define a selection which is as symmetric as possible between  $K_L$  and  $K_S$  decays, the variable  $p_T'$  is used, defined as the component of the kaon momentum orthogonal to the line joining the production target and the point where the kaon trajectory crosses the plane of the first drift chamber. To select  $\pi^+\pi^-$  candidates, the cut  $p_T'^2 < 2 \times 10^{-4}$  GeV $^2/c^2$  is applied.

The time of the  $\pi^+\pi^-$  decay is determined from hits in the scintillator hodoscope associated with the tracks and has a resolution of  $\sim 150$  ps. The events with insufficient information to determine the decay time accurately are discarded. This inefficiency is 0.1% and is measured to be equal for  $K_S$  and  $K_L$ .

#### 4.3. $K_S$ tagging

A decay is labelled  $K_S$  if a coincidence is found (within a  $\pm 2$  ns interval) between its event time and a proton time measured by the Tagger. Fig. 1 shows the time distributions for  $K_S$  and  $K_L$  decays to  $\pi^+\pi^-$  which have been identified as such by their vertex positions in the vertical direction. A similar procedure

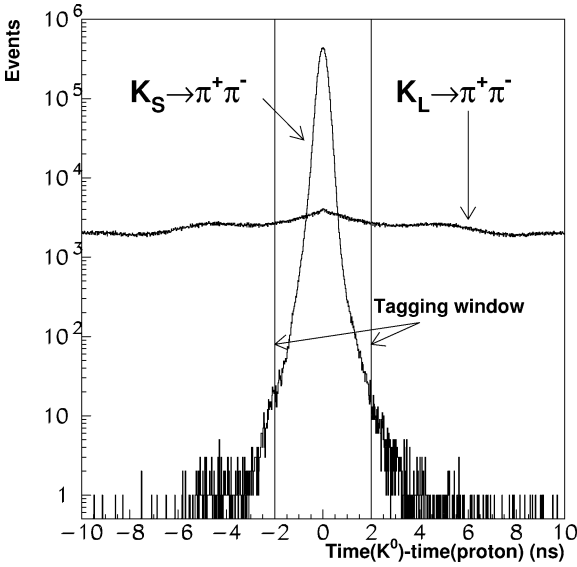


Fig. 1. Time coincidence for  $K_S$  and  $K_L$   $\pi^+\pi^-$  decays, identified by their reconstructed vertex.

is not possible for  $\pi^0\pi^0$  decays; therefore tagging provides the only way to distinguish  $K_S$  from  $K_L$ . The selection of  $K_S$  and  $K_L$  samples is done by means of tagging for both the  $\pi^+\pi^-$  and  $\pi^0\pi^0$  modes, so that systematic effects are mostly symmetric.

The probability that a  $K_S$  decay is assigned to the  $K_L$  beam, due to coincidence inefficiencies, is denoted by  $\alpha_{SL}$ . This tagging inefficiency is directly measured in the  $\pi^+\pi^-$  mode, using the vertical vertex position, and is  $(1.12 \pm 0.03) \times 10^{-4}$ , dominated by the Tagger inefficiency. The inefficiency could be different for  $\pi^+\pi^-$  and  $\pi^0\pi^0$  decays, since different detectors are used. The difference between the two modes is estimated using a large sample of  $K_S$  and  $K_L$  decays into  $2\pi^0$  and  $3\pi^0$  where one of the photons converts into an electron–positron pair. The time from the LKr clusters can then be compared with the scintillator-hodoscope time from the two tracks. The conclusion is that the  $\pi^0\pi^0$  and  $\pi^+\pi^-$  tagging inefficiencies agree within an uncertainty of  $\pm 0.5 \times 10^{-4}$ , which corresponds to an uncertainty on  $R$  of  $\pm 3 \times 10^{-4}$ . The tagging inefficiency can also be measured directly in  $\pi^0\pi^0$  events with a subsequent  $\pi^0 \rightarrow e^+e^-\gamma$  Dalitz decay, which allows the  $K_S$  to be identified from the two-track vertex. However this method is statistically limited. Another cross-check is performed in special

runs where only  $K_S$  are present; it gives a tagging inefficiency in agreement with the result above.

The probability that a  $K_L$  decay is identified as a  $K_S$  decay due to an accidental coincidence between the event and a proton is called accidental tagging and is denoted as  $\alpha_{LS}$ . It is measured in the  $\pi^+\pi^-$  mode to be  $(8.115 \pm 0.010) \times 10^{-2}$ .<sup>16</sup> The  $\alpha_{LS}$  difference,  $\Delta\alpha_{LS}$ , between the  $\pi^0\pi^0$  and  $\pi^+\pi^-$  modes is estimated by measuring the probability to find a proton within time windows 4 ns wide, located before or after the event time in tagged  $K_L$  events (i.e., events with no proton in coincidence). Ten windows are chosen, centred at 5 ns intervals from the event time so as to follow the 200 MHz structure of the proton beam. The extrapolation from the side windows to the coincidence window is performed in the  $\pi^+\pi^-$  mode with vertex-selected  $K_L$  and in the  $\pi^0\pi^0$  mode using  $3\pi^0$  decays, which come almost entirely from the  $K_L$  beam (the very small contribution from the  $K_S$  beam being subtracted). The measured value of  $\Delta\alpha_{LS} = \alpha_{LS}^{00} - \alpha_{LS}^{\pm\pm} = (+3.4 \pm 1.4) \times 10^{-4}$  corresponds to a correction on  $R$  of  $(+6.9 \pm 2.8) \times 10^{-4}$ . The origin of this effect is discussed in Section 6.2.

#### 4.4. Definition of the decay region

The fiducial ranges in kaon energy  $E_K$  and in proper time  $\tau$  used to count events are chosen to be  $70 < E_K < 170$  GeV and  $0 < \tau < 3.5\tau_S$ , where  $\tau = 0$  is defined at the position of the AKS counter and  $\tau_S$  is the  $K_S$  mean lifetime. For  $K_L$  events, the decay time cut is applied on reconstructed  $\tau$ , while for  $K_S$  events the cut at  $\tau = 0$  is applied using the AKS to veto decays occurring upstream. The nominal  $\tau = 0$  positions defined by the AKS differ by  $21.0 \pm 0.5$  mm between  $\pi^+\pi^-$  and  $\pi^0\pi^0$  decays. The veto inefficiency is 0.36% for  $\pi^0\pi^0$  events and 0.22% for  $\pi^+\pi^-$  decays. Given the fractions of decays occurring upstream of the AKS position (respectively 5.8% and 4.0%), the correction to be applied to the double ratio is  $(1.2 \pm 0.3) \times 10^{-4}$ .

$K_S \rightarrow \pi\pi$  decays can be produced in both beams by scattering of beam particles in the collimators and, in the case of the  $K_S$  beam, in the AKS counter. To

<sup>16</sup> It was  $(10.649 \pm 0.008) \times 10^{-2}$  in the 1998–1999 data sample.

reduce this contamination, a cut on the extrapolated kaon impact point at the level of the LKr calorimeter is applied to all events. For  $\pi^0\pi^0$  decays, it is defined as the energy-weighted average  $x, y$  positions of the four showers at the face of the LKr calorimeter. For  $\pi^+\pi^-$  decays, it is the momentum-weighted average position of the tracks measured upstream of the spectrometer magnet and projected onto the face of the LKr calorimeter. The extrapolated kaon impact point is required to be within 10 cm of the intersecting beam axes. The radii of the  $K_L$  and  $K_S$  beam spots are respectively 3.6 cm and 4.6 cm, so effects related to resolution smearing are negligible.

#### 4.5. Data quality selection

Data collected in the  $\pi^+\pi^-$  mode are affected by an overflow condition in the drift chambers which resets the front-end readout buffers when there are more than seven hits in a plane within a 100 ns time interval. This occurs mostly when an accidental particle generates an electromagnetic shower upstream of the spectrometer and sprays the drift chambers with particles. To maintain the highest reconstruction and trigger efficiencies, events used in the analysis are required to have no overflows within  $\pm 312$  ns of the event time. To minimise possible effects of  $K_L/K_S$  intensity variation and to equalise the beam intensities seen by good events, this requirement is applied to both  $\pi^+\pi^-$  and  $\pi^0\pi^0$  decays. The resulting event loss is 11% in the 2001 data sample. This is significantly smaller than the 20% loss observed in the 1998–1999 data, due to the lower instantaneous beam intensity and to smaller noise in the drift chambers. Other dead time conditions affecting the first and the second level  $\pi^+\pi^-$  trigger ( $\approx 0.3\%$ <sup>17</sup>) are also recorded and applied in the analysis to  $\pi^0\pi^0$  decays.

Because of large beam intensity variations at the very beginning of the spill, data from the first 0.2 s are not used in the analysis. The corresponding loss of events is  $\approx 1\%$  and cancels in the ratio between  $\pi^0\pi^0$  and  $\pi^+\pi^-$  decays.

## 5. R corrections and systematic uncertainties

The data are divided into 20 bins in kaon energy, each 5 GeV wide. The numbers of  $K_S$  and  $K_L$  candidates are corrected for the mistagging probabilities discussed previously. The total numbers of events are  $1.546 \times 10^6$   $K_L \rightarrow \pi^0\pi^0$ ,  $2.159 \times 10^6$   $K_S \rightarrow \pi^0\pi^0$ ,  $7.136 \times 10^6$   $K_L \rightarrow \pi^+\pi^-$  and  $9.605 \times 10^6$   $K_S \rightarrow \pi^+\pi^-$ .

Corrections for trigger efficiencies, background subtractions and residual acceptance differences between  $K_L$  and  $K_S$  are applied separately in each energy bin before computing the average of  $R$ .

### 5.1. Trigger efficiencies

The  $\pi^0\pi^0$  trigger efficiency is measured using a control sample of events triggered by a scintillating fibre detector located inside the LKr calorimeter. The efficiency is found to be  $(99.901 \pm 0.015)\%$ . The small inefficiency is  $K_S-K_L$  symmetric and no correction to the double ratio need be applied.

The  $\pi^+\pi^-$  trigger efficiency is  $(98.697 \pm 0.017)\%$ .<sup>18</sup> The difference between the  $\pi^+\pi^-$  trigger efficiency for  $K_S$  and  $K_L$  decays is computed in each energy bin. The overall correction on the double ratio is  $(5.2 \pm 3.6) \times 10^{-4}$ , where the uncertainty is given by the statistics of the control samples used to measure the efficiency.

### 5.2. Backgrounds

#### 5.2.1. Background to the $\pi^0\pi^0$ mode

The background to the  $K_L \rightarrow \pi^0\pi^0$  signal comes uniquely from  $K_L \rightarrow 3\pi^0$  decays, while the  $K_S$  mode is background free. The  $K_L \rightarrow 3\pi^0$  background has a flat  $\chi^2$  distribution. To estimate this background, a control region is defined by  $36 < \chi^2 < 135$ . The excess of  $K_L$  candidates in this region over a Monte Carlo expectation for  $\pi^0\pi^0$  decays is used to extrapolate the background in the signal region. The Monte Carlo includes the effect of non-Gaussian tails in the calorimeter resolution so as to reproduce the observed distribution in the  $K_S$  sample.

<sup>18</sup> It was  $(97.782 \pm 0.021)\%$  in 1998–1999. The improvement comes from the lower beam intensity and the better efficiency of the drift chambers in 2001.

<sup>17</sup> It was 1.6% in the 1998–1999 data.

The background is subtracted from the  $K_L \rightarrow 2\pi^0$  sample in bins of kaon energy and the resulting correction on the double ratio, taking into account the uncertainties in the non-Gaussian tails and in the background extrapolation, is  $(-5.6 \pm 2.0) \times 10^{-4}$ .

### 5.2.2. Background to the $\pi^+\pi^-$ mode

The background from  $\Lambda \rightarrow p\pi^-$  in the  $K_S \rightarrow \pi^+\pi^-$  sample is negligible after the cut on the track momentum asymmetry.

The residual  $K_{e3}$  and  $K_{\mu3}$  backgrounds in the  $K_L$  sample are estimated by defining two control regions in the  $m_{\pi\pi}-p_T'^2$  plane. The first region,  $9.5 < (m_{\pi\pi} - m_K) < 19.0$  MeV/ $c^2$  and  $300 < p_T'^2 < 2000$  MeV $^2/c^2$ , is dominated by  $K_{e3}$  events, while the second,  $-17.0 < (m_{\pi\pi} - m_K) < -12.0$  MeV/ $c^2$  and  $300 < p_T'^2 < 500$  MeV $^2/c^2$ , contains roughly equal numbers of  $K_{e3}$  and  $K_{\mu3}$  events.

The background distributions in the control regions are modelled by a  $K_{e3}$  sample, selected with  $E/p > 0.95$ , and by a  $K_{\mu3}$  sample, obtained by reversing the muon veto requirement; the tails in the  $K_L \rightarrow \pi^+\pi^-$  distribution are estimated from the  $K_S$  sample. The result is then extrapolated to the signal region.

The overall  $K_{e3}$  background fraction is  $10.5 \times 10^{-4}$ , the  $K_{\mu3}$  background is  $4.0 \times 10^{-4}$ . The background subtraction is applied in bins of kaon energy and the resulting correction on the double ratio is  $(14.2 \pm 3.0) \times 10^{-4}$ , where the error has been estimated by changing the control regions and the modelling of the resolution tails.

Kaon decays to  $\pi^+\pi^-\gamma$  have been shown to have a negligible effect on  $R$  [8].

### 5.2.3. Collimator scattering

In the  $K_S$  beam, the cut on the extrapolated kaon impact point is stronger than the  $p_T'^2$  cut applied to  $\pi^+\pi^-$  decays, and therefore the contribution of beam scattering is removed symmetrically from both final states. On the contrary, in the  $K_L$  beam, the  $p_T'^2$  cut which is applied only in the  $\pi^+\pi^-$  mode is stronger and therefore the small residual contribution from scattered events must be subtracted from the  $\pi^0\pi^0$  sample.

The correction for this asymmetry is computed from reconstructed  $K_L \rightarrow \pi^+\pi^-$  candidates with an inverted  $p_T'^2$  cut. The scattered events are extracted

from the peak at the kaon mass in the  $m_{\pi\pi}$  invariant mass distribution. The correction to  $R$  is applied in bins of energy and it amounts to  $(-8.8 \pm 2.0) \times 10^{-4}$ .

### 5.3. Acceptance

The  $K_S$  and  $K_L$  acceptances are made very similar in both modes by weighting  $K_L$  events according to their proper decay time. The weighting factor takes into account the small interference term. A small difference in acceptances remains, related to the differences in  $K_S$  and  $K_L$  beam sizes and directions. This residual correction is computed using a large-statistics Monte Carlo simulation ( $4 \times 10^8$  generated kaon decays per mode). The largest contribution to the correction comes from the difference between the  $K_S$  and  $K_L$  beams near the beam axes in the spectrometer for  $\pi^+\pi^-$  decays. The acceptance correction related to the  $\pi^0\pi^0$  mode is small.

The systematic uncertainty on the acceptance correction is evaluated by varying the  $K_S$  beam halo, the beam positions and shapes, and the drift-chamber inefficiencies. The resulting systematic uncertainty is  $\pm 3.0 \times 10^{-4}$ . A detailed comparison between a fast simulation and a GEANT [21] based simulation of the spectrometer was performed on the 1998–1999 sample. This resulted in an additional systematic uncertainty of  $\pm 2.3 \times 10^{-4}$ . The final correction to  $R$  for the acceptance is:  $\Delta R(\text{acceptance}) = (+21.9 \pm 3.5(\text{MCstat}) \pm 4.0(\text{syst})) \times 10^{-4}$ .

### 5.4. Energy and distance scales

The determinations of the kaon energy, the decay vertex and the proper time in the  $\pi^0\pi^0$  mode rely on measurements of the photon energies and positions with the calorimeter.

The absolute energy scale is adjusted using  $K_S \rightarrow \pi^0\pi^0$  decays. The energy scale is set such that the average value of the reconstructed decay position in a range centred around the anticounter matches the value found in a Monte Carlo simulation. This measurement of the energy scale is checked using data taken during special runs (so-called  $\eta$  runs) with a  $\pi^-$  beam striking two thin targets located near the beginning and the end of the fiducial decay region, producing  $\pi^0$  and  $\eta$  with known decay positions. From two-photon decays of  $\pi^0$  and  $\eta$ , the reconstructed

vertex position can be computed using the  $\pi^0$  or the  $\eta$  mass value (the  $\eta$  mass value is taken from [20]), and compared to the nominal target positions. Continuum production of  $2\pi^0$  events is also used, with the advantage that the final state is very similar to the one of kaon decays. The two targets give energy scales consistent to better than  $10^{-4}$ . The uncertainty on the overall energy scale is estimated from these comparisons to be  $\pm 3 \times 10^{-4}$ . The corresponding uncertainty on the double ratio is  $\pm 2 \times 10^{-4}$ .

Non-linearities in the energy response are studied using  $K_{e3}$  decays, where the electron energy measured in the calorimeter can be compared to the momentum measured in the spectrometer, and using data from the  $\eta$  runs. Parameterising the deviations from linearity as  $\Delta E/E = \alpha/E + \beta E$ ,  $\alpha$  is constrained to  $\pm 10$  MeV and  $\beta$  is bound to be in the range  $\pm 2 \times 10^{-5} \text{ GeV}^{-1}$ . Taking also into account larger deviations from linearity observed in the region  $E_\gamma < 6$  GeV, the resulting uncertainty on the double ratio is  $\pm 3.8 \times 10^{-4}$ .

The uniformity of the calorimeter response over its surface is optimised using  $K_{e3}$  decays and checked using  $\pi^0$  decays from the  $\eta$  runs. Bias on the double ratio can arise from a dependence of the energy response on the photon impact radius  $r$ . Parameterising this effect as  $\Delta E/E = \gamma r$ ,  $\gamma$  can be bound to be in the range  $\pm 10^{-3} \text{ m}^{-1}$ . In the region close to the beam tube, residual variations are smaller than 0.2%. The systematic uncertainty on the double ratio from these effects is  $\pm 1.6 \times 10^{-4}$ .

Uncertainties in the correction of energy leakage from one cluster to another can lead to an apparent non-linearity and bias the double ratio. The correction used in the data is based on the transverse shower-profile measured during special runs in which single monochromatic electrons were sent to the calorimeter. The uncertainty in the shower profile is taken to be the difference between this measurement and the prediction of the GEANT Monte Carlo simulation. The resulting uncertainty on the double ratio is  $\pm 1.1 \times 10^{-4}$ .

The measurements of photon positions and the transverse size-scale of the calorimeter are adjusted and checked using  $K_{e3}$  decays, comparing the reconstructed cluster position with the electron track impact point extrapolated to the calorimeter. The associated uncertainty on the double ratio is  $\pm 1.6 \times 10^{-4}$ .

In the computation of the decay vertex position, the photon positions must be extrapolated to the

longitudinal position of the maximum of the shower to account correctly for deviations of the photon directions from the projectivity of the calorimeter. Comparing data and Monte Carlo simulation in  $K_{e3}$  decays, the uncertainty on this position is  $\pm 2$  cm. The resulting uncertainty on the double ratio is  $\pm 1.6 \times 10^{-4}$ .

Finally, the effect of non-Gaussian tails in the energy response is minimised by the choice of the procedure used to adjust the overall energy scale. Residual effects are investigated by applying to the Monte Carlo samples a parameterisation of non-Gaussian tails in the energy response (arising mostly from photo-production of hadrons early in the electromagnetic shower) derived from  $K_{e3}$  and  $\eta$  data. No bias on the double ratio is observed within the Monte Carlo statistical error which is  $\pm 1.0 \times 10^{-4}$ .

Adding all the above uncertainties in quadrature, the total systematic error on the double ratio from the measurements of the photon energies and positions is found to be  $\pm 5.3 \times 10^{-4}$ .

For  $\pi^+\pi^-$  decays, the vertex position is measured from the reconstructed tracks and is completely determined by the detector geometry. As a check, the reconstructed anticounter position can be measured in  $K_S \rightarrow \pi^+\pi^-$  decays. The value obtained agrees with the nominal position to better than 1 cm.<sup>19</sup> Uncertainties in the geometry of the detector are at the level of 2 mm for the distance between the first two drift chambers, and  $20 \mu\text{m}/\text{m}$  for their relative transverse scale. This corresponds to possible deviations of  $\approx \pm 2$  cm on the reconstructed AKS position. The corresponding uncertainty on the double ratio measurement is  $\pm 2.0 \times 10^{-4}$ . The asymmetry in the  $K_S$  and  $K_L$  event losses, which could arise from the effect of non-Gaussian tails in the  $p_T'^2$  resolution, is smaller than  $2.0 \times 10^{-4}$ . The overall uncertainty on the double ratio from the reconstruction of  $\pi^+\pi^-$  decays is therefore  $\pm 2.8 \times 10^{-4}$ .

## 6. Intensity effects

### 6.1. Uncertainty on $R$ due to accidental effects

Most of the accidental activity in the detector is related to kaon decays in the high-intensity  $K_L$  beam.

<sup>19</sup> The difference was 2 cm in the 1998–1999 data.

The overlap of extra particles with a good event may result in the loss of the event in the reconstruction or the selection,<sup>20</sup> depending on the time and space separation of the activity in the detector. This effect is minimised by the simultaneous collection of data in the four channels and by the fact that  $K_S$  and weighted  $K_L$  decays illuminate the detector in a similar way. The possible residual effect on the double ratio can be separated into two components: intensity variations between the two beams coupled to different, intensity-dependent, event losses in the  $\pi^+\pi^-$  and  $\pi^0\pi^0$  modes (intensity difference), and a residual difference in the illumination between  $K_S$  and  $K_L$  decays coupled to a variation of the event loss with the impact points of the  $K^0$  decay products (illumination difference).

### 6.1.1. Intensity difference

If the losses depend, as expected, linearly on the  $K_L$  beam intensity, the intensity difference effect is given by:

$$\Delta R = \Delta\lambda \frac{\Delta I}{I}, \quad (5)$$

where  $\Delta\lambda$  is the difference between the mean losses in  $\pi^+\pi^-$  and  $\pi^0\pi^0$ , and  $\Delta I/I$  is the difference in the mean  $K_L$  beam intensity as seen by  $K_L$  and  $K_S$  events.

The accidental rate can be measured directly from the activity in the detector within the readout time-window before each event. Comparing the rate of out-of-time LKr clusters and out-of-time tracks in good  $K_S, K_L \rightarrow \pi^+\pi^-$  decays,  $\Delta I/I$  is found to be respectively  $(+0.4 \pm 0.4)\%$  and  $(+0.6 \pm 0.3)\%$ , where the quoted uncertainties are only statistical. For this measurement  $K_S$  and  $K_L$  are identified by the decay vertex position to avoid the correlation between mistagging probability and beam intensity. The bias on  $\Delta I/I$  from the fact that this measurement uses good reconstructed decays is a negligible second-order effect. The measurement of accidental activity is illustrated in Fig. 2.

The  $K_L$  beam intensity for each event can also be estimated using the information from the  $K_L$  beam monitor, integrating the intensity over a 200 ns time window. The difference between the average intensities as seen by  $K_S$  and  $K_L$  decays is found to

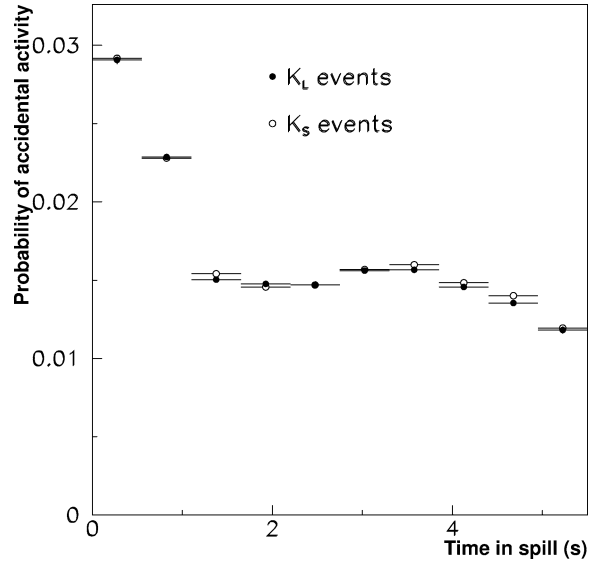


Fig. 2. Probability of accidental activity in the LKr in the  $\approx 150$  ns readout window, as a function of the time during the spill, for  $K_S$  and  $K_L$  decays to  $\pi^+\pi^-$ .

be  $(-0.08 \pm 0.04)\%$ , where the quoted uncertainty is only statistical. The systematic uncertainty on this measurement is estimated to be less than 1%. Another method to study the correlation of the two beams, which does not rely on the use of good events, consists of a direct computation of the correlation between the  $K_L$  and  $K_S$  beam monitor counts, using events taken uniformly in time. To avoid statistical fluctuations in the rate measurements, this is done using a 15  $\mu$ s integration time of the beam monitors. All known  $K_L/K_S$  variations take place on a much longer time scale. This method confirms that  $\Delta I/I$  is consistent with 0 within 1%. The final estimate for  $\Delta I/I$  is  $(0 \pm 1)\%$ .

The beam-induced event losses can be evaluated by overlaying data with beam monitor (BM) triggers taken in proportion to the beam intensity, which reproduce the ambient activity as seen by the detectors. Detector information from the original events and the BM triggers are superimposed at the raw-data level and the overlaid events undergo the standard reconstruction and analysis procedure. Losses and gains from migration of events around the cuts are taken into account. When estimating the event losses related to accidental activity, the losses related to doubling the noise effect inherent in this procedure must be removed. The net

<sup>20</sup> The losses in the trigger are already accounted for in the measurement of the trigger efficiency.

event losses induced by the accidental activity are at the level of 1 to 2%. The dominant source of event loss is found to be the appearance of the drift chamber overflow condition in the overlaid event. This loss is higher for  $\pi^+\pi^-$  decays than for  $\pi^0\pi^0$  because of the presence of at least two drift chamber hits per plane for the original  $\pi^+\pi^-$  decay. From this procedure,  $\Delta\lambda$  is found to be 1.0%. The overlay procedure can also be applied starting from a Monte Carlo sample of original  $\pi^+\pi^-$  and  $\pi^0\pi^0$  decays. In this case,  $\Delta\lambda$  is found to be 0.65%. The statistical uncertainties on  $\Delta\lambda$  from the overlay samples are less than 0.1%. The difference between the two estimates is attributed to the lower hit-multiplicity in the Monte Carlo samples compared to the data.

$\Delta\lambda$  can also be estimated directly from the data, by comparing the ratio of  $\pi^+\pi^-$  and  $\pi^0\pi^0$  events obtained in the normal  $K_L + K_S$  beam runs and in pure  $K_S$  runs, in which the accidental activity is one order of magnitude smaller. This leads to  $\Delta\lambda = (0.9 \pm 0.6)\%$ . Similarly,  $\Delta\lambda$  can be checked by dividing the data into bins of  $K_L$  beam intensity and looking at the variations in the ratio of  $\pi^+\pi^-$  and  $\pi^0\pi^0$  events. This leads to an estimate in agreement with the values above. In conclusion, from this study the final estimate of  $\Delta\lambda$  is  $(1.0 \pm 0.5)\%$ . This value is typically 30% lower than the estimate derived for the 1998–1999 data-taking period, as expected from the lower beam intensity in 2001.

Finally, the linearity of the losses with intensity can be checked by looking at the losses as a function of the beam intensity given by the BM triggers. Fig. 3 shows the accidental event losses in the  $\pi^+\pi^-$  and  $\pi^0\pi^0$  modes as a function of the beam intensity from the overlay procedure applied to Monte Carlo events.

Taking into account all the above results, the estimate of the uncertainty on the double ratio related to differences in intensity-dependent losses is  $\pm 1.1 \times 10^{-4}$ .<sup>21</sup>

### 6.1.2. Illumination difference

The illumination-difference effect has been estimated from the overlay samples, computing separately the losses for  $K_S$  and  $K_L$  events. This computation

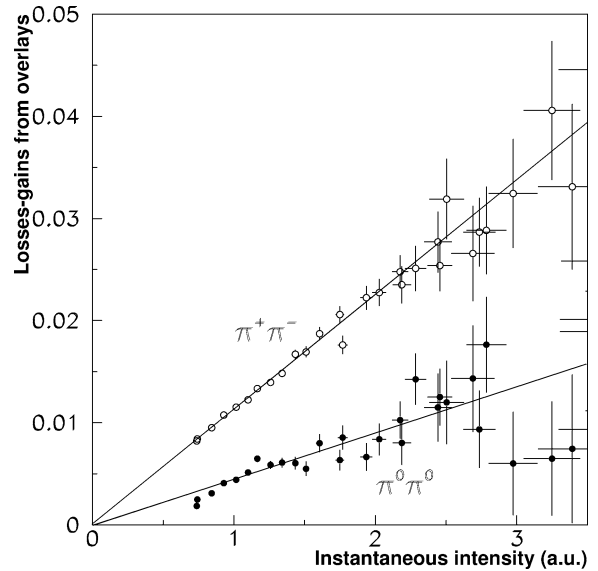


Fig. 3. Beam-induced net event losses as a function of instantaneous intensity in arbitrary units. Lines are drawn to guide the eyes.

has been performed using both data and Monte Carlo original events. In the first case, the value obtained is  $(+0.9 \pm 3.5) \times 10^{-4}$ , in the second it is  $(+1.4 \pm 2.8) \times 10^{-4}$ , where the quoted uncertainties are the statistical errors from the overlay samples. As expected, there is no evidence of a significant effect, and we use as uncertainty on the double ratio  $\pm 3.0 \times 10^{-4}$ .

### 6.1.3. Overall uncertainty on $R$ and cross-check

Combining the two above uncertainties in quadrature, the total uncertainty on  $R$  from accidental effects is  $\pm 3.1 \times 10^{-4}$ . This uncertainty is dominated by the statistical error of the overlay procedure.

The overlay method can also be used to estimate the combination of the two effects. For this,  $K_S$  events are overlaid only with BM triggers from the  $K_S$  monitor and  $K_L$  events only with BM triggers from the  $K_L$  monitor. This method relies on the accuracy of the BM triggers to estimate correctly the  $K_L$ – $K_S$  intensity difference. From this method, the overall accidental effect on the double ratio is found to be  $(4.7 \pm 4.9) \times 10^{-4}$ , where the quoted error is the statistical uncertainty from the overlay sample. The systematic uncertainty from the accuracy of the BM triggers is expected to be  $< 2 \times 10^{-4}$ . From this cross-check, there is no evidence of any unexpected effect on the double ratio.

<sup>21</sup> For the 1998–1999 sample, this uncertainty was estimated to be  $\pm 3.0 \times 10^{-4}$ .

#### 6.1.4. In-time activity from the $K_S$ target

The techniques above do not take into account any additional detector activity in the  $K_S$  beam generated by the same proton which produced the  $K_S$  event. Studies of this background, mostly searching in the LKr calorimeter for additional clusters in  $2\pi^0$  events from pure  $K_S$  beam runs, allow an upper bound on the effect on  $R$  of  $1 \times 10^{-4}$  to be set.

#### 6.2. Origin of $\Delta\alpha_{LS}$

The accidental tagging probability  $\alpha_{LS}$  depends only on the proton beam intensity seen by the Tagger and, consequently, it is to first order the same for  $\pi^0\pi^0$  and  $\pi^+\pi^-$ . However, because the event selection is more sensitive to accidentals for  $\pi^+\pi^-$  events, we expect a difference of the measured  $\alpha_{LS}$  for the  $\pi^0\pi^0$  and  $\pi^+\pi^-$  samples due to beam-intensity variations with time. A quantitative understanding of the effect of accidental activity on selected events can be reached by studying the BM trigger overlays.

A value  $\Delta\alpha_{LS} = (+3.5 \pm 0.4) \times 10^{-4}$  is expected from the overlay of data, where the error is only statistical. Using loss and gain probabilities from the overlay Monte Carlo samples instead of data we find  $\Delta\alpha_{LS} = (+2.0 \pm 0.4) \times 10^{-4}$ .

In Fig. 4 the variation of  $\Delta\alpha_{LS}$  within the spill is

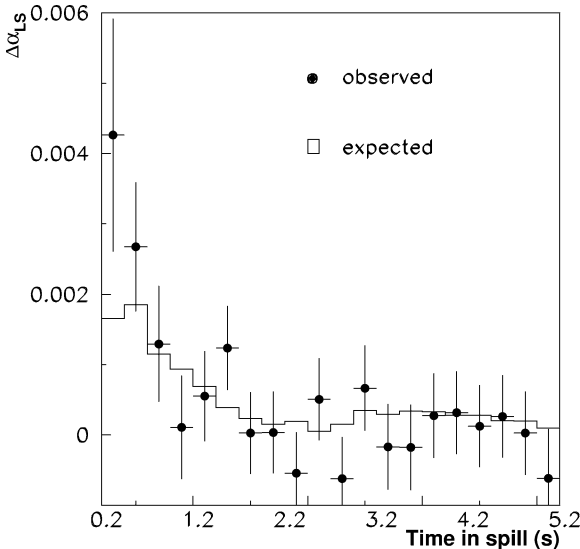


Fig. 4. Measured compared to predicted values of  $\Delta\alpha_{LS}$  as a function of the time during the spill.

shown and compared with the overlay computation. Most of the difference in accidental tagging between the  $\pi^0\pi^0$  and  $\pi^+\pi^-$  modes comes from the beginning of the spill where the instantaneous intensity is higher and the beam intensity variations more significant.

Another source of event losses is the inefficiency of the  $\pi^+\pi^-$  trigger. The intensity-dependent part is studied separately and its effect on  $\Delta\alpha_{LS}$  is estimated to be  $(0.4 \pm 0.2) \times 10^{-4}$ .

The observed  $\Delta\alpha_{LS}$  value of  $(+3.4 \pm 1.4) \times 10^{-4}$  is therefore well reproduced both qualitatively and quantitatively.

## 7. Result

The effect on the result of the corrections described above, and the various sources of systematic uncertainties are summarised in Table 1.

Fig. 5 shows the measured double ratio after corrections as a function of the kaon energy.

The final result for the double ratio from the 2001 data set is  $R = 0.99181 \pm 0.00147 \pm 0.00110$ , where the first error is the statistical error from the  $2\pi$  samples, and the second is systematic. Out of this systematic uncertainty,  $\pm 0.00065$  is due to the finite statistics of the control samples used to study the systematic effects.

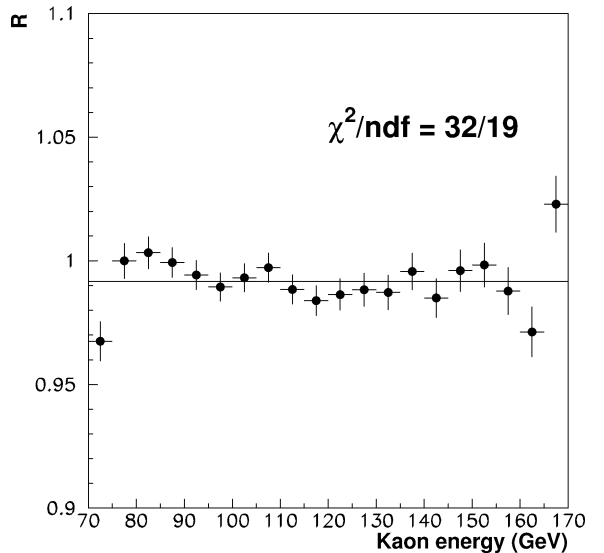


Fig. 5. Measured double ratio  $R$  in kaon energy bins.

Table 1  
Corrections and systematic uncertainties on the double ratio  $R$  (2001 data)

		in $10^{-4}$	
$\pi^+\pi^-$ trigger inefficiency	+5.2	$\pm 3.6$	(stat)
AKS inefficiency	+1.2	$\pm 0.3$	
Reconstruction of $\pi^0\pi^0$	–	$\pm 5.3$	
Reconstruction of $\pi^+\pi^-$	–	$\pm 2.8$	
Background to $\pi^0\pi^0$	–5.6	$\pm 2.0$	
Background to $\pi^+\pi^-$	+14.2	$\pm 3.0$	
Beam scattering	–8.8	$\pm 2.0$	
Accidental tagging	+6.9	$\pm 2.8$	(stat)
Tagging inefficiency	–	$\pm 3.0$	
Acceptance statistical	+21.9	$\pm 3.5$	(stat)
Acceptance systematic	+21.9	$\pm 4.0$	
Accidental activity intensity difference	–	$\pm 1.1$	
Accidental activity illumination difference	–	$\pm 3.0$	(stat)
$K_S$ in time activity	–	$\pm 1.0$	
Total	+35.0	$\pm 11.0$	

Many cross-checks of the stability of the result have been performed, by varying some of the selection cuts and by searching for a dependence of the result on several variables, such as the beam intensity, the time during the spill, and the data-taking period. No significant variation in the result is observed. An analysis adopting a different scheme for data compaction, filtering, selection and correction procedures was also performed in addition to the one presented here. Its result fully confirms the above measurement.

The corresponding value of the direct CP-violation parameter  $\text{Re}(\epsilon'/\epsilon)$  from formula (1) is:

$$\text{Re}(\epsilon'/\epsilon) = (13.7 \pm 2.5 \pm 1.1 \pm 1.5) \times 10^{-4},$$

where the first uncertainty is the pure statistical error from the  $2\pi$  samples, the second is the systematic error coming from the statistics of the control samples, and the third is the contribution of the other systematic uncertainties. Combining the errors in quadrature, the result is:

$$\text{Re}(\epsilon'/\epsilon) = (13.7 \pm 3.1) \times 10^{-4}.$$

This result is in good agreement with the published value from the 1997–1999 data:  $\text{Re}(\epsilon'/\epsilon) = (15.3 \pm 2.6) \times 10^{-4}$ .

The comparison of the present and earlier results is particularly significant since they were obtained from data taken at different average beam intensities. The correlated systematic uncertainty between the two results is estimated to be  $\pm 1.4 \times 10^{-4}$ . Taking this

correlation into account, the combined, final result on  $\text{Re}(\epsilon'/\epsilon)$  from the NA48 experiment is:

$$\text{Re}(\epsilon'/\epsilon) = (14.7 \pm 1.4 \pm 0.9 \pm 1.5) \times 10^{-4},$$

or, with combined errors:

$$\text{Re}(\epsilon'/\epsilon) = (14.7 \pm 2.2) \times 10^{-4}.$$

## Acknowledgements

It is a pleasure to thank the technical staff of the participating laboratories and universities for their efforts in the design and construction of the apparatus, in the operation of the experiment, and in the processing of the data.

## References

- [1] J.H. Christenson, et al., Phys. Rev. Lett. 13 (1964) 138.
- [2] B. Aubert, et al., Phys. Rev. Lett. 87 (2001) 091801; K. Abe, et al., Phys. Rev. Lett. 87 (2001) 091802.
- [3] M. Kobayashi, K. Maskawa, Prog. Theor. Phys. 49 (1973) 652.
- [4] M. Ciuchini, G. Martinelli, Nucl. Phys. B (Proc. Suppl.) 99 (2001) 27; E. Pallante, et al., Nucl. Phys. B 617 (2001) 441; A.J. Buras, et al., Nucl. Phys. B 592 (2001) 55; Y.L. Wu, Phys. Rev. D 64 (2001) 0106001; S. Bertolini, et al., Phys. Rev. D 63 (2001) 056009; J. Donoghue, in: F. Costantini, et al. (Eds.), Proc. Int. Conference on Kaon Physics, in: Frascati Physics Serie, Vol. 26, 2001, p. 93;

- T. Hambye, et al., Nucl. Phys. B 564 (2000) 391;  
J. Bijnens, J. Prades, JHEP 0006 (2000) 035;  
T. Blum, et al., hep-lat/0108013;  
J.I. Noaki, et al., hep-lat/0110075.
- [5] G. Barr, et al., Phys. Lett. B 317 (1993) 233.  
[6] L.K. Gibbons, et al., Phys. Rev. Lett. 70 (1993) 1203.  
[7] V. Fanti, et al., Phys. Lett. B 465 (1999) 335.  
[8] A. Lai, et al., Eur. Phys. J. C 22 (2001) 231.  
[9] A. Glazov, KTeV Collaboration, in: F. Costantini, et al. (Eds.), Proc. Int. Conference on Kaon Physics, in: Frascati Physics Serie, Vol. 26, 2001, p. 115.  
[10] A. Alavi-Harati, et al., Phys. Rev. Lett. 83 (1999) 22.  
[11] C. Biino, et al., CERN-SL-98-033(EA), in: Proceedings of 6th EPAC, Stockholm, 1998, IOP, 1999, p. 2100.  
[12] N. Doble, L. Gagnon, P. Grafström, Nucl. Instrum. Methods B 119 (1996) 181.  
[13] P. Graftström, et al., Nucl. Instrum. Methods A 344 (1994) 487; H. Bergauer, et al., Nucl. Instrum. Methods A 419 (1998) 623.  
[14] R. Moore, et al., Nucl. Instrum. Methods B 119 (1996) 149.  
[15] D. Bédèrede, et al., Nucl. Instrum. Methods A 367 (1995) 88; I. Augustin, et al., Nucl. Instrum. Methods A 403 (1998) 472.  
[16] G.D. Barr, et al., Nucl. Instrum. Methods A 370 (1993) 413.  
[17] G. Unal, NA48 Collaboration, in: B. Aubert, et al. (Eds.), Proc. IX Int. Conf. on Calorimetry in HEP, in: Frascati Physics Serie, Vol. 21, 2001, p. 361.  
[18] G. Barr, et al., Nucl. Instrum. Methods A 485 (2002) 676.  
[19] S. Anvar, et al., Nucl. Instrum. Methods A 419 (1998) 686.  
[20] A. Lai, et al., Phys. Lett. B 533 (2002) 196.  
[21] GEANT Description and Simulation Tool, CERN Program Library Long Writeup W5013 (1994).